

Article

Preparation and Characteristics of γ -Fe₂O₃/Polyaniline-Curcumin Composites

Yongli Li, Chunxia Zhu and Jinqing Kan *

School of Chemistry and Chemical Engineering, Yangzhou University, Yangzhou 225002, China; E-Mails: 15705279695@163.com (Y.L.); zcx_740@163.com (C.Z.)

* Author to whom correspondence should be addressed; E-Mail: jqkan@yzu.edu.cn; Tel.: +86-514-8797-5590 (ext. 9415); Fax: +86-514-8797-5590 (ext. 8410).

Academic Editor: Bruno Schmaltz

Received: 18 November 2015 / Accepted: 11 December 2015 / Published: 17 December 2015

Abstract: Superparamagnetic nanomaterials are showing great prospects in medical treatments with targeting medicines. A new conductive superparamagnetic nanocomposite, γ -Fe₂O₃/polyaniline-curcumin (γ -Fe₂O₃/PANI-curcumin), was prepared by using the interaction between an amino group in polyaniline and a ketone group in curcumin. The γ -Fe₂O₃/PANI-curcumin nanocomposite showed superparamagnetism (30 emu g⁻¹) and electrochemical activity, based on the results of magnetization curve and cyclic voltammetry (CV). Transmission electron microscope (TEM) indicated that the particle size of γ -Fe₂O₃/PANI-curcumin was between 10 and 50 nm. Fourier transform infrared spectra (FT-IR) and X-ray diffraction (XRD) were used to characterize the γ -Fe₂O₃/PANI-curcumin nanocomposite, confirming that curcumin was immobilized into the γ -Fe₂O₃/PANI chain. This study provided an academic foundation for developing a new material for immobilizing an anticancer drug.

Keywords: curcumin; maghemite; nanocomposites; polyaniline; superparamagnetism

1. Introduction

In the 1980s, the invention of a conducting polymer changed the traditional understanding that a polymer was only an insulator [1]. Their magnetic composites have become extremely attractive because of their unique and intriguing properties and promising industrial applications [2–7], such as electrical

and magnetic shielding, nonlinear optics, molecular electronics, electrochemical power sources [8], drugs [9], sensors and microwave absorbents [10–12].

Polyaniline (PANI) nanoparticles containing γ -Fe₂O₃ (thereafter written as γ -Fe₂O₃/PANI) is a novel nanomaterial exhibiting a promising application in medical treatments as a targeting drug carrier. Not only γ -Fe₂O₃/PANI can diminish the particle size, but also polyaniline provides functional groups for loading drugs. The γ -Fe₂O₃/PANI nanoparticles could show a core-shell structure and superparamagnetism as well as high environmental and thermal stabilities [13]. Up to date, γ -Fe₂O₃/PANI has mostly been prepared by chemical methods [14–16]. One of the main ingredients of γ -Fe₂O₃/PANI, polyaniline (PANI), known for more than 150 years, is the oldest and one of the commonly used conducting polymers due to its easiness of synthesis, environmental stability, and unique reversible properties of doping/dedoping or redox [17]. In particular, polyaniline has a good biological compatibility. MacDiarmid *et al.* [18] observed that the conductivity of polyaniline can last about 100 h in the human body and current on conductor surface can control a shape and function of anchorage-dependent cells. Mattioli-Belmonte used polyaniline as an electroactive polymer in the culture of excitable cells and opened the possibility of using this material as an electroactive scaffold in cardiac and neuronal tissues as well as demonstrated that PANI was biocompatible in long-term *in vivo* animal studies [19].

Another main ingredient of γ -Fe₂O₃/PANI, γ -iron sesquioxide (γ -Fe₂O₃), has been attractive due to its non-toxicity, thermal and chemical stabilities, and low cost. It has been regarded as a valuable material to mollify biologically active compounds, bio-tag drug molecules, and hysteretically heat maligned cells. Its magnetism allows a manipulation with external fields [20–22]. Therefore, γ -Fe₂O₃ is a good candidate used for drug delivery, information storage, bioseparation, magnetic sensors, and catalysts.

Curcumin is a phenolic pigment extracted from the rhizome of *curcuma longa*, which as a natural medicine has various derivatives. Curcumin with antineoplastic, anti-oxidation, and anti-inflammation functions is the main composition of *curcuma longa*, a kind of traditional Chinese medicine, which can also adjust immunity and has extensive value both in economic and medical aspects.

In this article, we developed a new process to synthesize the composite of γ -Fe₂O₃/PANI-curcumin. Its electrical and magnetic properties were investigated. The curcumin can be immobilized into polyaniline chains based on the interaction between an amino group of polyaniline and a ketone group of curcumin. The results from Fourier transform infrared spectra (FT-IR) and X-ray diffraction (XRD) confirmed that curcumin was immobilized into PANI chains. CV and magnetization studies showed that the composite had both superparamagnetism and electrochemical activities.

2. Materials

All chemicals used were of analytical grade. Aniline and ammonium persulfate (APS) were purchased from the Shanghai Chemical Reagent Co., Ltd. (Shanghai, China). Aniline was distilled under reduced pressure and stored in the refrigerator at about 4 °C before a usage. Ferrous sulfate heptahydrate (FeSO₄·7H₂O), ferric chloride hexahydrate (FeCl₃·6H₂O), ethanol and ammonium hydroxide (30 wt. % of NH₃ in water) were obtained from the Sinopharm Chemical Reagent Co., Ltd. (Shanghai, China). Curcumin was purchased from the Shanghai Aladdin Reagent Co., Ltd. (Shanghai, China). Other chemicals were used as received without a further treatment. All of the aqueous solutions were prepared with doubly distilled water.

2.1. Preparation of γ -Fe₂O₃ Nanoparticles

The γ -Fe₂O₃ nanoparticles were prepared according to published procedures [23–27] with some modifications. For a typical example, 5.4 g of FeCl₃·6H₂O (20 mmol) and 2.8 g of FeSO₄·7H₂O (10 mmol) were dissolved in 20 and 10 mL of water, respectively. The two solutions were mixed, and then dripped into 400 mL of 0.6 mol dm⁻³ aqueous ammonia solution for over 20 min with constant stirring. The pH values of the reaction mixture were maintained between 11 and 12 with an addition of a concentrated ammonium hydroxide solution. The products were separated by a magnet, repeatedly washed with doubly distilled water, and then air dried at 80 °C for 12 h.

2.2. Preparation of γ -Fe₂O₃/PANI

A typical procedure for preparing γ -Fe₂O₃/PANI was as follows [23]. 1.9 mL of aniline (20 mmol) was dissolved in 200 mL of 0.5 mol dm⁻³ HCl with the suspended γ -Fe₂O₃. Then 0.5 mol dm⁻³ APS (20 mmol) was added slowly into above solution and stirred for 5 h. The γ -Fe₂O₃/PANI suspension was centrifuged (Model 80-2, 4000 r min⁻¹, Jintan Hongkai instrument factory, Jintan, China), washed successively with double-distilled water and ethanol, and vacuum dried at 70 °C for 12 h. In order to obtain the γ -Fe₂O₃/PANI base, the prepared γ -Fe₂O₃/PANI was immersed in 0.2 mol dm⁻³ aqueous ammonium with magnetic stirring for 24 h, filtrated and washed with double-distilled water to a pH of 6–7, and vacuum dried at 80 °C for 12 h.

2.3. Preparation of a γ -Fe₂O₃/PANI-Curcumin Composite

With a different ratio of γ -Fe₂O₃/PANI and curcumin, curcumin was dissolved in ethanol, and then γ -Fe₂O₃/PANI was added into the curcumin solution. The mixed solution reacted under an ultrasonic water bath for hours. The γ -Fe₂O₃/PANI-curcumin was washed with ethanol and vacuum dried at 70 °C for 12 h, then pulverized after being dried for characterizations.

3. Characterization of Samples

FT-IR spectra of the samples with pressed KBr pellets were recorded on a Bruker Tensor 27 FT-IR spectrometer (Ettlingen, Germany) in the range of 4000–400 cm⁻¹. X-ray diffraction patterns of powder samples were taken on an XD-3A powder diffractometer using a Cu K α radiation ($\lambda = 1.5406 \text{ \AA}$) to measure a crystallinity. The applied magnetic field dependence of magnetization was obtained on a vibrating sample magnetometer (VSM) (ADE Co., Lowell, MA, USA) in a field ranging from –8000 to 8000 Oe at room temperature. The size and morphology of the resulting particles were imaged by using a Tecnai-12 (FEI Electron Optics, Eindhoven, The Netherlands) transmission electron microscope. The cyclic voltammogram (CV) was taken on a CHI 660 electroanalysis workstation (Chenhua Instrument Co, Shanghai, China). The cell consisted of a working electrode (6 × 6 mm²), a platinum sheet (10 × 10 mm²) counter electrode and a saturated calomel electrode (SCE) as a reference electrode in a Britton-Robinson (B-R) buffer (pH 7.0). The working electrode was prepared by dispersing the samples in DMF and then dripping the resultant suspension onto the platinum sheet, which was then dried in atmosphere. Samples were dispersed in the aqueous PVP solution under

an ultrasonic water bath for 30 min, and the particle sizes were obtained from the Zetasizer Nano instrument (Malvern Instruments Ltd., Worcestershire, UK).

4. Results and Discussion

It is well known that aldehydes and ketones can react readily with equimolar amounts of primary amines and yield imines [28]. Curcumin and polyaniline contain ketones and end groups of primary amine, respectively. We envision the synthetic route of γ -Fe₂O₃/polyaniline-curcumin (γ -Fe₂O₃/PANI-curcumin) as follows (Figure 1):

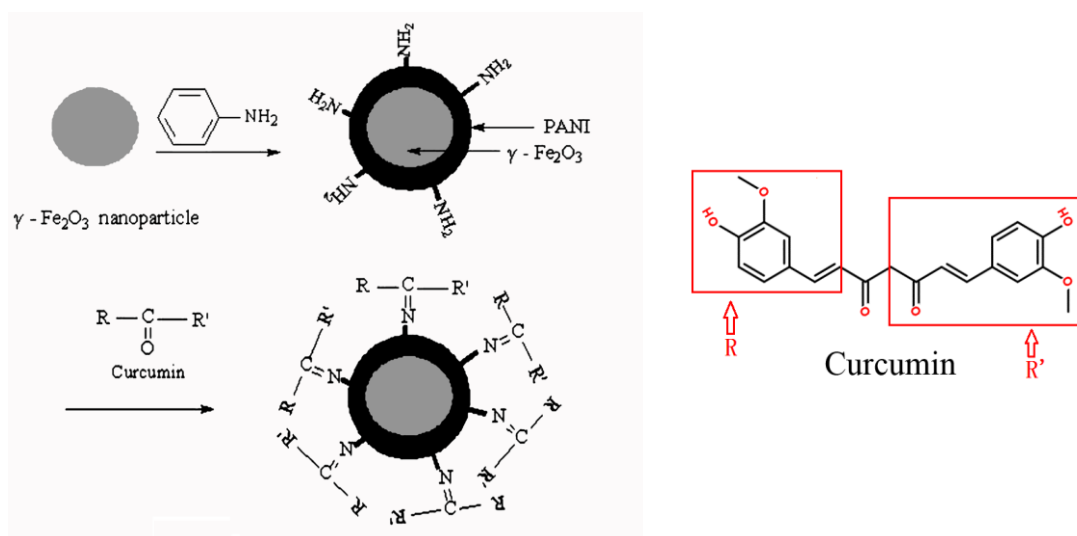


Figure 1. Schematic illustration for formation of γ -Fe₂O₃/PANI-curcumin.

Step 1: preparation of the skeleton material: we coated a layer of polyaniline on the prepared γ -Fe₂O₃ particles by a method of solution polymerization, forming a γ -Fe₂O₃/PANI composite with a core-shell structure.

Step 2: immobilization of curcumin: curcumin was immobilized into the outer layer of PANI, which was due to an interaction between a carbonyl group of curcumin and an amino group of polyaniline.

4.1. IR Spectra of Samples

Figure 2 shows the IR spectra of γ -Fe₂O₃, γ -Fe₂O₃/PANI, γ -Fe₂O₃/PANI-curcumin and curcumin. The peaks at 1590 and 1503 cm⁻¹ corresponded to the C=C stretching vibration of the quinoid ring and the benzene ring, respectively. The peak at 1303 cm⁻¹ attributed to aromatic (C–N) stretching band of polyaniline. The peak at 1128 cm⁻¹ corresponded to B–NH–B, where B refers to the benzenic-type rings. The peaks of γ -Fe₂O₃/PANI-curcumin virtually overlapped with that of polyaniline over 1128 cm⁻¹. Compared Curve c with Curve b in Figure 2, it can be seen that there were two new peaks at 1029 and 962 cm⁻¹ in Curve c, which were the same with the peaks of curcumin in the Curve d. It indicated that curcumin was immobilized into γ -Fe₂O₃/PANI, forming γ -Fe₂O₃/PANI-curcumin. For the formation of a new –N=C bond, it can be verified by comparing the intensity ratio of γ -Fe₂O₃/PANI-curcumin (c) at 1590 and 1503 cm⁻¹, because the characteristic peak of –N=C bond was

approximately the same with that of C=C stretching at 1590 cm^{-1} . The intensity ratio of $\gamma\text{-Fe}_2\text{O}_3/\text{PANI}$ -curcumin (c) could be stronger than that of $\gamma\text{-Fe}_2\text{O}_3/\text{PANI}$ (b) at 1590 and 1503 cm^{-1} . This also showed that the new -N=C bond was formed due to the interaction between an amino group of polyaniline and a ketone group of curcumin.

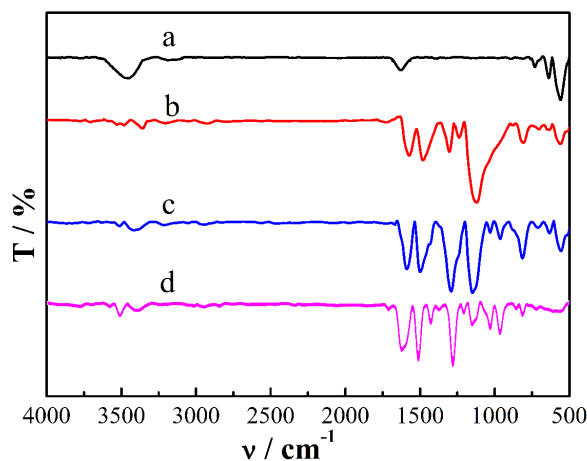


Figure 2. IR spectra of samples: a, $\gamma\text{-Fe}_2\text{O}_3$; b, $\gamma\text{-Fe}_2\text{O}_3/\text{PANI}$; c, $\gamma\text{-Fe}_2\text{O}_3/\text{PANI}$ -curcumin; and d, curcumin.

Figure 3 showed FT-IR spectra of $\gamma\text{-Fe}_2\text{O}_3/\text{PANI}$ -curcumin with different molar ratios of $\gamma\text{-Fe}_2\text{O}_3/\text{PANI}$ to curcumin at room temperature. Molar ratios of Curves a, b and c are 1:2, 1:1, and 2:1, respectively. In Figure 4, three samples appeared the characteristic peak of Fe-O stretching vibration at 570 cm^{-1} , this indicated that the $\gamma\text{-Fe}_2\text{O}_3$ existed in three samples. It can be seen from Figure 3 that the peak position of $\gamma\text{-Fe}_2\text{O}_3/\text{PANI}$ -curcumin with different molar ratios of $\gamma\text{-Fe}_2\text{O}_3/\text{PANI}$ to curcumin was the same, indicating that the molar ratios of $\gamma\text{-Fe}_2\text{O}_3/\text{PANI}$ to curcumin barely affected the molecular structure.

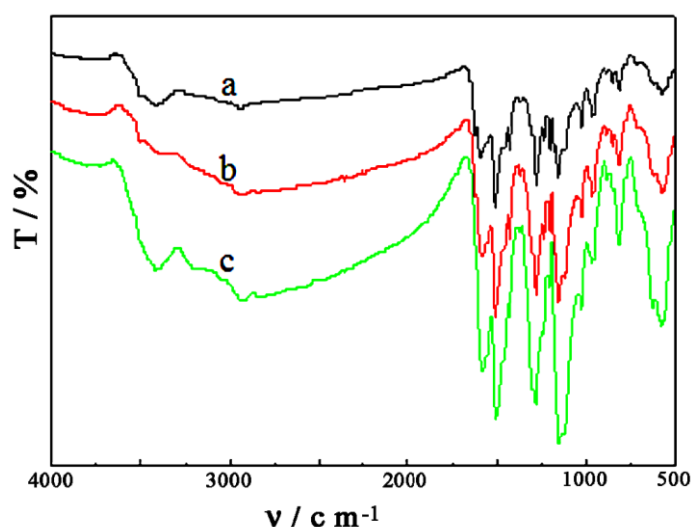


Figure 3. FT-IR spectra of $\gamma\text{-Fe}_2\text{O}_3/\text{PANI}$ -curcumin with different molar ratios between $\gamma\text{-Fe}_2\text{O}_3/\text{PANI}$ and curcumin: $\gamma\text{-Fe}_2\text{O}_3/\text{PANI}$:curcumin = (a) 1:2; (b) 1:1; and (c) 2:1.

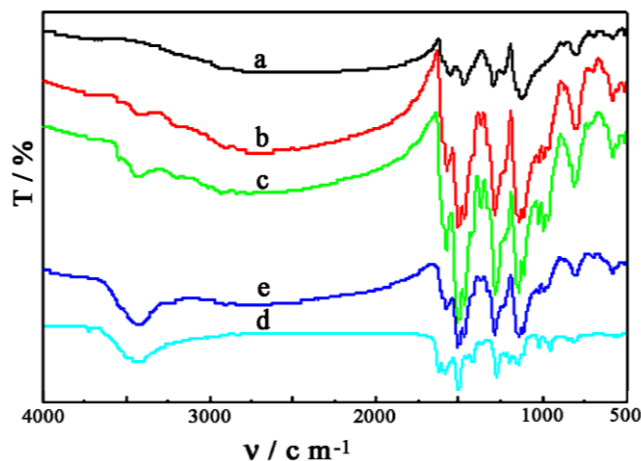


Figure 4. IR spectra of samples with different reaction times at room temperature: (a) 4 h; (b) 8 h; (c) 12 h; (d) 16 h and (e) 20 h.

Figure 4 was IR spectra of the samples with different reaction time at room temperature, and shows that different reaction time had an insignificant effect on the structure of the samples as their peak positions were roughly the same.

4.2. Magnetic Characterization of the Samples

Figure 5 showed the dependence of the external magnetic field on magnetization for γ -Fe₂O₃ (a), γ -Fe₂O₃/PANI (b), and γ -Fe₂O₃/PANI-curcumin (c) in the range of -8000 to 8000 Oe at room temperature. It was found from Figure 5 that the saturated magnetization (M_s) of γ -Fe₂O₃, γ -Fe₂O₃/PANI, and γ -Fe₂O₃/PANI-curcumin decreased gradually as forming the PANI shell and immobilizing curcumin. The following sequence was observed: γ -Fe₂O₃ (83 emu g^{-1}) > γ -Fe₂O₃/PANI (44 emu g^{-1}) > γ -Fe₂O₃/PANI-curcumin (34 emu g^{-1}). The saturated magnetization of γ -Fe₂O₃/PANI-curcumin mainly came from that of γ -Fe₂O₃. The gradually decreasing saturated magnetization from γ -Fe₂O₃ to γ -Fe₂O₃/PANI-curcumin indicated the decrease of the γ -Fe₂O₃ content in unit mass products, which also further confirmed that γ -Fe₂O₃ was covered by PANI and curcumin was immobilized onto γ -Fe₂O₃/PANI. They were consistent with the results from IR (Figure 2). It can also be seen from Figure 5 that they all exhibited superparamagnetism because there was no remnant magnetization (M_r) or coercive force (H_c) [29].

In order to determine the most suitable proportion of curcumin during synthesizing γ -Fe₂O₃/PANI-curcumin, γ -Fe₂O₃/PANI-curcumin was prepared by using different molar ratios of γ -Fe₂O₃/PANI to curcumin. Figure 6 showed the magnetizations of γ -Fe₂O₃/PANI-curcumin with different molar ratios of γ -Fe₂O₃/PANI to curcumin. Curve a was γ -Fe₂O₃/PANI, its saturated magnetization was 44 emu g^{-1} . Curves b, c and d represented that of the different molar ratios of γ -Fe₂O₃/PANI to curcumin, which were 2:1, 1:2, and 1:1, respectively. It can be seen from Figure 6 that the saturated magnetization intensity of γ -Fe₂O₃/PANI-curcumin nanoparticles reduced with increasing the molar ratios of γ -Fe₂O₃/PANI to curcumin. This may be due to that curcumin was immobilized into γ -Fe₂O₃/PANI leading to the decrease of the γ -Fe₂O₃ content in unit mass products. From Figure 6 we can also understand that the saturated magnetization intensity was various for different molar ratios

prepared products. When the molar ration between γ -Fe₂O₃/PANI and curcumin is 2:1, the saturated magnetization (41 emu g⁻¹) was maximum. When the molar ratios between γ -Fe₂O₃/PANI and curcumin was 1:2 and 1:1, the saturated magnetization decrease from 41 emu g⁻¹ to 24 emu g⁻¹ and 19 emu g⁻¹, respectively. In the figure, we can also obtain that all γ -Fe₂O₃/PANI-curcumin were superparamagnetic, so we can infer the particle size of ferromagnetic samples was very small and less than 90 nm. Because when the size of the particles ($d = 14\text{--}90$ nm) was within a critical dimension of superparamagnetic, many ferromagnetic substances would transform from the ferromagnetism into superparamagnetism [30].

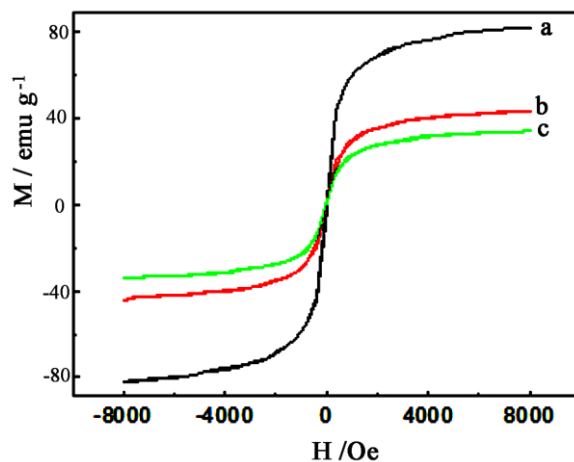


Figure 5. Dependence of magnetization on the applied magnetic field at room temperature for samples: a, γ -Fe₂O₃; b, γ -Fe₂O₃/PANI and c, γ -Fe₂O₃/PANI/curcumin.

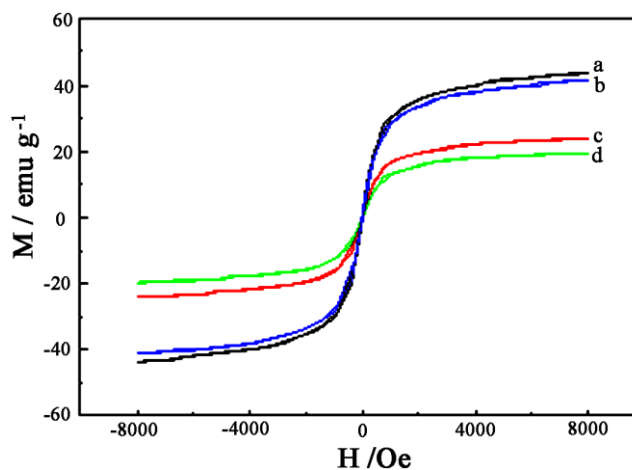


Figure 6. The magnetic hysteresis plots for γ -Fe₂O₃/PANI-curcumin with different molar ratios between γ -Fe₂O₃/PANI and curcumin: a, γ -Fe₂O₃/PANI; b, 2:1; c, 1:2 and d, 1:1.

Figure 7 showed the VSM of γ -Fe₂O₃/PANI-curcumin under the different reaction time at room temperature, the Curves a~e were the hysteresis loops of γ -Fe₂O₃/PANI-curcumin corresponding to the reaction time of 4, 8, 12, 16, and 20 h, respectively. From Figure 7 we can find γ -Fe₂O₃/PANI-curcumin were all superparamagnetic at different reaction time, indicating that the particle diameter of γ -Fe₂O₃/PANI-curcumin was less than 50 nm. Figure 8 showed magnetizations of γ -Fe₂O₃/PANI-curcumin were affected by the reaction time. During the reaction time between 4 and 16 h, the saturated

magnetization decreased with the increase of the reaction time. The strongest saturated magnetization was 30 emu g^{-1} at 4 h, and the weakest one was 13 emu g^{-1} at 16 h. This trend may be attributed to the increase of the curcumin percentage in the composite as the reaction time increased. It should be noticed that the saturated magnetization for 20 h was greater than that at 16 h, which did not follow the trend and needed to be further studied.

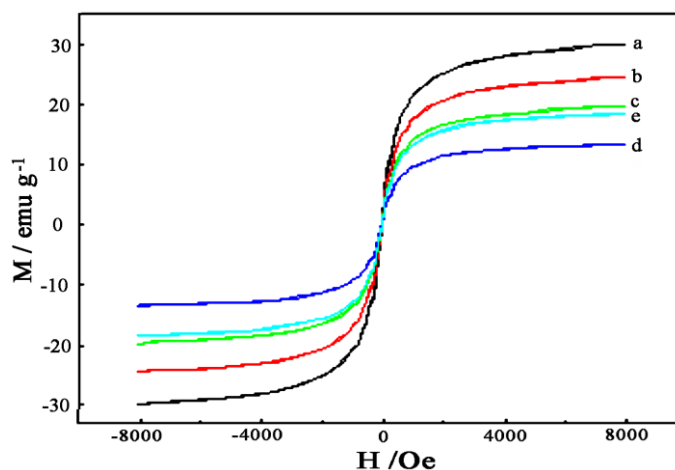


Figure 7. The magnetic hysteresis plots for $\gamma\text{-Fe}_2\text{O}_3/\text{PANI}/\text{curcumin}$ under the different reaction time: a, 4 h; b, 8 h; c, 12 h; d, 16 h and e, 20 h.

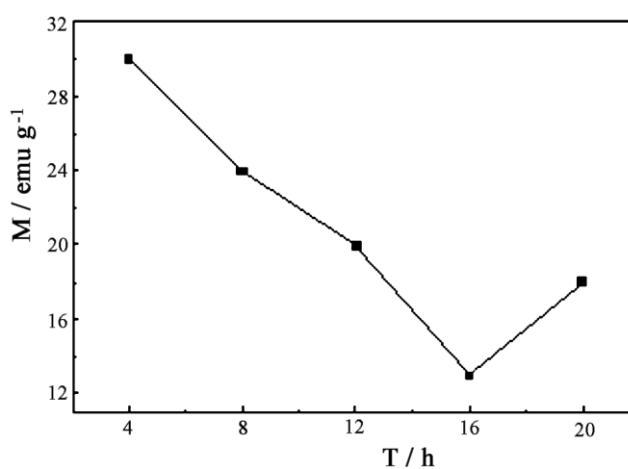


Figure 8. Diagram of magnetization *versus* reaction time for $\gamma\text{-Fe}_2\text{O}_3/\text{PANI}\text{-curcumin}$.

4.3. TEM and Particle Size Distribution Images of Samples

Figure 9 showed a TEM image of $\gamma\text{-Fe}_2\text{O}_3/\text{PANI}\text{-curcumin}$ and the particle size distribution of $\gamma\text{-Fe}_2\text{O}_3$ (a), $\gamma\text{-Fe}_2\text{O}_3/\text{PANI}$ (b), and $\gamma\text{-Fe}_2\text{O}_3/\text{PANI}\text{-curcumin}$ (c). It can be seen from the TEM image that the average particle diameter of $\gamma\text{-Fe}_2\text{O}_3/\text{PANI}\text{-curcumin}$ was between 10 and 50 nm. However, the particle size obtained from the Zetasizer Nano instrument was smaller than that from TEM, the reason could be from that the equal refractive index of the hydration layer of the particles and the solvent, the hydration layer was not detected in the Zetasizer Nano instrument. The obtained particle size was smaller than that from TEM. The particle diameter was within the critical dimension of superparamagnetism ($d = 14\text{--}90 \text{ nm}$), they were consistent with the result of the VSM. The conductive

superparamagnetic particles with a diameter less than 100 nm were expected to be highly favorable as a targeting carrier for a local therapy [31].

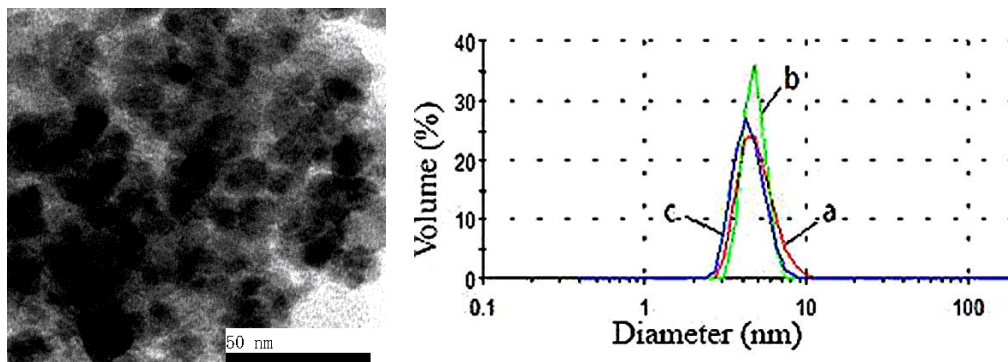


Figure 9. TEM image of $\gamma\text{-Fe}_2\text{O}_3/\text{PANI}$ -curcumin and the particle size distribution image of $\gamma\text{-Fe}_2\text{O}_3$ (a), $\gamma\text{-Fe}_2\text{O}_3/\text{PANI}$ (b) and $\gamma\text{-Fe}_2\text{O}_3/\text{PANI}$ -curcumin (c).

4.4. Cyclic Voltammograms of Composite Particles

The cyclic voltammogram of the samples was measured in a BR buffer solution and shown in Figure 10. Curves a–c represented the CVs of polyaniline, $\gamma\text{-Fe}_2\text{O}_3/\text{PANI}$, and $\gamma\text{-Fe}_2\text{O}_3/\text{PANI}$ -curcumin, respectively. It can be clearly seen that when the film mass was settled, the electrochemical activity of $\gamma\text{-Fe}_2\text{O}_3/\text{PANI}$ significantly decreased, this might be due to the decrease of the polyaniline content in $\gamma\text{-Fe}_2\text{O}_3/\text{PANI}$. It also can be seen from Figure 10 that $\gamma\text{-Fe}_2\text{O}_3/\text{PANI}$ -curcumin still possessed some electrochemical activity in a BR buffer solution, which may be favorable to the shape and function of anchorage-dependent cells under current on conductor surface.

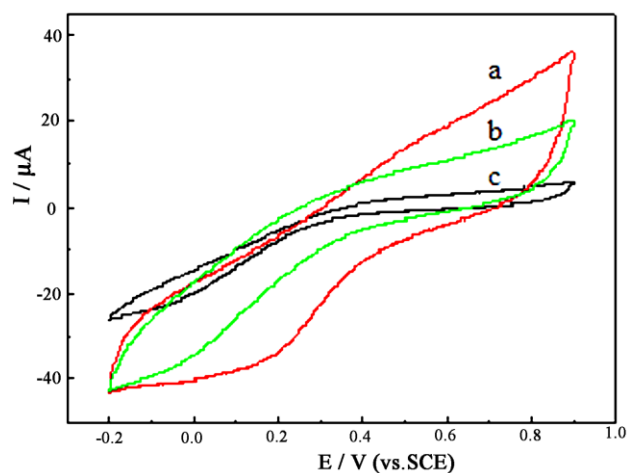


Figure 10. The cyclic voltammograms of samples: a, PANI; b, $\gamma\text{-Fe}_2\text{O}_3/\text{PANI}$ and c, $\gamma\text{-Fe}_2\text{O}_3/\text{PANI}$ /curcumin.

4.5. X-ray Diffraction of Samples

Figure 11 showed the X-ray diffraction patterns of $\gamma\text{-Fe}_2\text{O}_3$, $\gamma\text{-Fe}_2\text{O}_3/\text{PANI}$ and $\gamma\text{-Fe}_2\text{O}_3/\text{PANI}$ -curcumin. The $\gamma\text{-Fe}_2\text{O}_3$ in Curve b had a XRD pattern with diffraction peaks of $2\theta = 30.2^\circ$, 35.6° , 43.2° , 53.8° , 57.3° and 62.9° , which was well consistent with the standard pattern of the crystalline $\gamma\text{-Fe}_2\text{O}_3$ in

Curve a. Comparing Curve b with c, the pattern of the γ -Fe₂O₃ component were unchanged. The additional peaks at 20.4 ° and 25.2 ° in Curve c came from the characteristic crystalline nature of PANI. When curcumin was immobilized onto γ -Fe₂O₃/PANI, the obvious crystal diffraction peak at 14 °–28 ° disappeared (Curve d). It may be due to the reason that the interaction between functional groups of curcumin and polyaniline affected the crystal form of PANI. Meanwhile, the characteristic signal of γ -Fe₂O₃ significantly decreased, which indicated that the interaction between curcumin and polyaniline decreased the content of γ -Fe₂O₃ in the product.

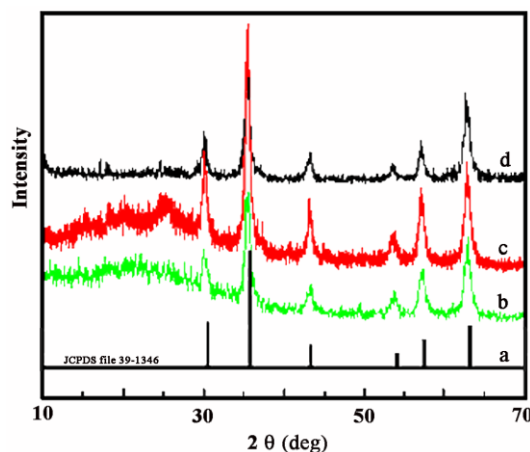


Figure 11. XRD patterns of samples: a, standard spectrum of γ -Fe₂O₃; b, γ -Fe₂O₃; c, γ -Fe₂O₃/PANI and d, γ -Fe₂O₃/PAIN/curcumin.

5. Conclusions

A conductive superparamagnetic nanocomposite (γ -Fe₂O₃/PANI-curcumin) was synthesized in this study. Various characterizations of γ -Fe₂O₃/PANI-curcumin validated its great electrochemical activity and stable magnetic conductivity. The composite particles had a diameter between 10 and 50 nm, and shows promise as a drug carrier. The reaction time of 4 h and the molar ratio of 2:1 between curcumin and γ -Fe₂O₃/PANI were found to be the optimal conditions, generating the strongest magnetism. This magnetic nanocomposite was expected to be a good candidate for manipulating drugs to a specific location in a target therapy.

Acknowledgments

This project was supported by the National Science Foundation of China (No. 20873119), and by the Priority Academic Program Development of Jiangsu Higher Education Institutions. Part of the data was from the Testing Center of the Yangzhou University.

Author Contributions

Jinqing Kan came up with the conception and design; Yongli Li and Chunxia Zhu did the collection and assembly of data; all three authors completed the data analysis and interpretation, and drafted the manuscript. Jinqing Kan final approved of the manuscript.

Conflicts of Interest

The authors declare no conflict of interest.

References

1. Galvin, M.E.; Wnek, G.E. Electrically conductive polymer composites: Polymerization of acetylene in polyethylene. *Polymer* **1982**, *23*, 795–797.
2. Pu, Z.; Zhou, X.; Yang, X.; Jia, K.; Liu, X. One step grafting of iron phthalocyanine containing flexible chains on Fe₃O₄ nanoparticles towards high performance polymer magnetic composites. *J. Magn. Magn. Mater.* **2015**, *385*, 368–376.
3. Held, G.A.; Grinstein, G.; Doyle, H.; Sun, S.; Murray, C.B. Competing interactions in dispersions of superparamagnetic nanoparticles. *Phys. Rev. B* **2001**, doi:10.1103/PhysRevB.64.012408.
4. Qiu, Y.; Ma, Z.; Hu, P. Environmentally benign magnetic chitosan/Fe₃O₄ composites as reductant and stabilizer for anchoring Au NPs and their catalytic reduction of 4-nitrophenol. *J. Mater. Chem. A* **2014**, *2*, 13471–13478.
5. Urbanova, V.; Magro, M.; Gedanken, A.; Baratella, D.; Vianello, F.; Zboril, R. Nanocrystalline iron oxides, composites, and related materials as a platform for electrochemical, magnetic, and chemical biosensors. *Chem. Mater.* **2014**, *26*, 6653–6673.
6. Jiang, W.; Chen, X.; Wu, J.; Xu, S.; Tian, R. Synthesis and evaluation of fluorescent magnetic composites as targeted drug delivery carriers. *J. Mater. Eng. Perform.* **2015**, *24*, 1237–1242.
7. Fang, F.F.; Liu, Y.D.; Choi, H.J. Electrorheological and magnetorheological response of polypyrrole/magnetite nanocomposite particles. *Colloid Polym. Sci.* **2013**, *291*, 1781–1786.
8. Ma, Z.; Kan, J. Study of cylindrical Zn/PANI secondary batteries with the electrolyte containing alkylimidazolium ionic liquid. *Synth. Met.* **2013**, *174*, 58–62.
9. Wuang, S.C.; Neoh, K.G.; Kang, E.T.; Pack, D.W.; Leckband, D.E. HER-2-mediated endocytosis of magnetic nanospheres and the implications in cell targeting and particle magnetization. *Biomaterials* **2008**, *29*, 2270–2279.
10. Kawaguchi, H. Functional polymer microspheres. *Prog. Polym. Sci.* **2000**, *25*, 1171–1210.
11. Gomez-Romero, P. Hybrid organic-inorganic materials—In search of synergic activity. *Adv. Mater.* **2001**, *13*, 163–174.
12. Xiao, H.M.; Zhang, W.D.; Wan, M.X.; Fu, S.Y. Novel electromagnetic functionalized γ -Fe₂O₃/polypyrrole composite nanostructures with high conductivity. *J. Polym. Sci. Polym. Chem.* **2009**, *47*, 4446–4453.
13. Deng, J.; Ding, X.; Zhang, W.; Peng, Y.; Wang, J.; Long, X.; Li, P.; Chan, A.S.C. Magnetic and conducting Fe₃O₄-cross-linked polyaniline nanoparticles with core-shell structure. *Polymer* **2002**, *43*, 2179–2184.
14. Huang, H.; Zhang, L.; Kan, J. γ -Fe₂O₃/polyaniline-Ionidamine prepared by doping/dedoping method. *Mater. Chem. Phys.* **2014**, *145*, 27–35.
15. Gao, R.; Li, J.; Han, S.; Wen, B.; Zhang, T.; Miao, H.; Zhang, Q. Magnetisation behaviour of mixtures of ferrofluids and paramagnetic fluids with same particle volume fractions. *J. Exp. Nanosci.* **2012**, *7*, 282–297.

16. Shen, Q.; Lang, J.; Kan, J. γ -Fe₂O₃@Polyaniline-Chlorambucil synthesized by using doping/dedoping method of polyaniline. *Asian J. Chem.* **2014**, *26*, 6492–6498.
17. Li, D.; Huang, J.X.; Kaner, R.B. Polyaniline nanofibers: A unique polymer nanostructure for versatile applications. *Acc. Chem. Res.* **2009**, *42*, 135–145.
18. Bidez, P.R.; Li, S.; MacDiarmid, A.G.; Venancio, E.C.; Wei, Y.; Lelkes, P.I. Polyaniline, an electroactive polymer, supports adhesion and proliferation of cardiac myoblasts. *J. Biomater. Sci. Polym. Ed.* **2006**, *17*, 199–212.
19. Mattioli-Belmonte, M.; Giavaresi, G.; Biagini, G.; Virgili, L.; Giacomini, M.; Fini, M.; Giantomassi, F.; Natali, D.; Torricelli, P.; Giardino, R. Tailoring biomaterial compatibility: *In vivo* tissue response versus *in vitro* cell behavior. *Int. J. Artif. Organs* **2003**, *26*, 1077–1085.
20. Layek, S.; Pandey, A.; Pandey, A.; Verma, H.C. Synthesis of γ -Fe₂O₃ nanoparticles with crystallographic and magnetic texture. *Int. J. Eng. Sci. Technol.* **2010**, *2*, 33–39.
21. Pankhurst, Q.A.; Connolly, J.; Jonesa, S.K.; Dobson, J. Applications of magnetic nanoparticles in biomedicine. *J. Phys. D Appl. Phys.* **2003**, *36*, 167–181.
22. Levy, M.; Wilhelm, C.; Siaugue, J.M.; Horner, O.; Bacri, J.C.; Gazeau, F. Magnetically induced hyperthermia: Size-dependent heating power of γ -Fe₂O₃ nanoparticles. *J. Phys. Condens. Matter* **2008**, *20*, 1–5.
23. Tang, B.Z.; Geng, Y.; Lam, J.W.Y.; Li, B.; Jing, X.; Wang, X.; Wang, F.; Pakhomov, A.B.; Zhang, X.X. Processible nanostructured materials with electrical conductivity and magnetic susceptibility: Preparation and properties of maghemite/polyaniline nanocomposite films. *Chem. Mater.* **1999**, *11*, 1581–1589.
24. Tang, B.Z.; Geng, Y.H.; Sun, Q.H.; Zhang, X.X.; Jing, X.B. Processible nanomaterials with high conductivity and magnetizability. Preparation and properties of maghemite/polyaniline nanocomposite films. *Pure Appl. Chem.* **2000**, *72*, 157–162.
25. Tang, R.; Liu, M.; Kan, J. Synthesis, characterisation, and conductive superparamagnetism studies of γ -Fe₂O₃/Polyaniline-Levodopa Composites. *Polym. Renew. Resour.* **2012**, *3*, 1–12.
26. Morales, M.P.; Veintemillas-Verdaguer, S.; Montero, M.I.; Serna, C.J. Surface and internal spin canting in γ -Fe₂O₃ nanoparticles. *Chem. Mater.* **1999**, *11*, 3058–3064.
27. Cao, S.W.; Zhu, Y.J.; Ma, M.Y.; Li, L.; Zhang, L. Hierarchically nanostructured magnetic hollow spheres of Fe₃O₄ and γ -Fe₂O₃: Preparation and potential application in drug delivery. *J. Phys. Chem. C* **2008**, *112*, 1851–1856.
28. Vančik, H. *Basic Organic Chemistry for the Life Sciences*; Springer International Publishing: New York, NY, USA, 2014; p. 94.
29. Bean, C.P.; Livingston, J.D. Superparamagnetism. *J. Appl. Phys.* **1959**, *30*, S120–S129.
30. Liu, J.; Wan, M.X. Composites of polypyrrole with conducting and ferromagnetic behaviors. *J. Polym. Sci. Polym. Chem.* **2000**, *38*, 2734–2739.
31. Olivier, J.C. Drug transport to brain with targeted nanoparticles. *NeuroRx* **2005**, *2*, 108–119.